

Air Force Institute of Technology

AFIT Scholar

Faculty Publications

4-22-2013

Reversible Mn Segregation at the Polar Surface of Lithium Tetraborate

Christina L. Dugan

Robert L. Hengehold
Air Force Institute of Technology

Stephen R. McHale

Juan A. Colon Santana

John W. McClory
Air Force Institute of Technology

See next page for additional authors

Follow this and additional works at: <https://scholar.afit.edu/facpub>



Part of the [Electromagnetics and Photonics Commons](#), [Engineering Physics Commons](#), and the [Semiconductor and Optical Materials Commons](#)

Recommended Citation

Dugan, C., et al. (2013). Reversible Mn segregation at the polar surface of lithium tetraborate. *Applied Physics Letters*, 102(16), 161602. <https://doi.org/10.1063/1.4802760>

This Article is brought to you for free and open access by AFIT Scholar. It has been accepted for inclusion in Faculty Publications by an authorized administrator of AFIT Scholar. For more information, please contact richard.mansfield@afit.edu.

Authors

Christina L. Dugan, Robert L. Hengehold, Stephen R. McHale, Juan A. Colon Santana, John W. McClory, Volodymyr T. Adamiv, Yaroslav V. Burak, Ya B. Losovyj, and Peter A. Dowben

Reversible Mn segregation at the polar surface of lithium tetraborate

Cite as: Appl. Phys. Lett. **102**, 161602 (2013); <https://doi.org/10.1063/1.4802760>

Submitted: 21 March 2013 . Accepted: 09 April 2013 . Published Online: 23 April 2013

Christina Dugan, Robert L. Hengehold, Steve R. McHale, Juan A. Colón Santana, John W. McClory, V. T. Adamiv, Ya. V. Burak, Ya. B. Losovyj, and Peter A. Dowben



View Online



Export Citation



CrossMark

ARTICLES YOU MAY BE INTERESTED IN

Identification of electron and hole traps in lithium tetraborate ($\text{Li}_2\text{B}_4\text{O}_7$) crystals: Oxygen vacancies and lithium vacancies

Journal of Applied Physics **107**, 113715 (2010); <https://doi.org/10.1063/1.3392802>

Electron and hole traps in Ag-doped lithium tetraborate ($\text{Li}_2\text{B}_4\text{O}_7$) crystals

Journal of Applied Physics **110**, 093719 (2011); <https://doi.org/10.1063/1.3658264>

Low-temperature crystal structure, specific heat, and dielectric properties of lithium tetraborate $\text{Li}_2\text{B}_4\text{O}_7$

Journal of Applied Physics **108**, 093524 (2010); <https://doi.org/10.1063/1.3504244>

Lock-in Amplifiers
up to 600 MHz



Zurich
Instruments



Reversible Mn segregation at the polar surface of lithium tetraborate

Christina Dugan,¹ Robert L. Hengehold,¹ Steve R. McHale,¹ Juan A. Colón Santana,² John W. McClory,¹ V. T. Adamiv,³ Ya. V. Burak,³ Ya. B. Losovyj,⁴ and Peter A. Dowben⁴

¹Department of Engineering Physics, Air Force Institute of Technology, 2950 Hobson Way, Wright Patterson Air Force Base, Ohio 45433-7765, USA

²Center for Energy Sciences Research, University of Nebraska-Lincoln, 230 Whittier Research Center, Lincoln, Nebraska 68583-0857, USA

³Institute of Physical Optics, 23 Dragomanov St., Lviv 79005, Ukraine

⁴Department of Physics and Astronomy and the Nebraska Center for Materials and Nanoscience, University of Nebraska-Lincoln, Theodore Jorgensen Hall, 855 North 16th Street, P.O. Box 8800299, Lincoln, Nebraska 68588-0299, USA

(Received 21 March 2013; accepted 9 April 2013; published online 23 April 2013)

We find Mn surface segregation for single crystals of Mn doped $\text{Li}_2\text{B}_4\text{O}_7$, nominally $\text{Li}_{1.95}\text{Mn}_{0.05}\text{B}_4\text{O}_7(001)$, but as the temperature increases, evidence of this Mn surface segregation diminishes significantly. At room temperature, the surface photovoltaic charging is significant for this pyroelectric material but is quenched at a temperature well below that seen for the undoped $\text{Li}_2\text{B}_4\text{O}_7$ samples. The suppression of surface charging in the region of 120°C that accompanies the temperature of Mn dissolution in the bulk of $\text{Li}_2\text{B}_4\text{O}_7$, i.e., the reversal of Mn surface segregation (215°C), suggests that along the (001) direction, ionic transport must be considered as significant. © 2013 AIP Publishing LLC [<http://dx.doi.org/10.1063/1.4802760>]

Although lithium tetraborate, $\text{Li}_2\text{B}_4\text{O}_7$, is both a pyroelectric and a dielectric,¹ along the (001) direction conductivity appears dominated by Li^+ transport.²⁻⁴ Investigations of the temperature dependence of conductivity have shown that the conductivity along the polar tetragonal c axis is much higher than along the orthogonal directions, perhaps by as much as five orders of magnitude.⁴⁻⁶ This should lead to some odd surface segregation effects, and we have chosen Mn doped $\text{Li}_2\text{B}_4\text{O}_7$ samples, nominally $\text{Li}_{1.95}\text{Mn}_{0.05}\text{B}_4\text{O}_7(001)$, to illustrate the facility by which surface segregation can occur at the polar surface of lithium tetraborate, $\text{Li}_2\text{B}_4\text{O}_7$.

The pyroelectric oxide lithium tetraborate, (space group $I4_1cd$), is a complex tetragonal crystal with 104 atoms per unit cell,^{4,7-11} as illustrated in the inset of Fig. 1. Recent investigations show that manganese atoms likely substitute at the boron sites, but occupation of the lithium sites remains possible.¹² In the former (B) sites, the local bonds are severely strained and in the latter (Li) case, the data would support a picture that involves large charge redistribution. Electron paramagnetic resonance (EPR) is a technique for studying chemical species that have one or more unpaired electrons. Prior EPR¹²⁻¹⁵ and optical¹⁵⁻¹⁸ investigations of the doped $\text{Li}_2\text{B}_4\text{O}_7:\text{Mn}$ single crystals and glasses have been interpreted as Mn entering the $\text{Li}_2\text{B}_4\text{O}_7$ lattice as Mn^{2+} ions, and into the $\text{Li}_2\text{B}_4\text{O}_7$ glass structure in the form of Mn^{2+} and Mn^{3+} . In most of the prior work, it has been suggested that the Mn dopant takes the place of Li^+ in a deformed tetrahedral oxygen environment. This Li^+ doping site for Mn would make Mn doping very similar to that of Ag in lithium tetraborate,¹⁹ but the luminescent data for lithium tetraborate doped with Mn, especially the x-ray luminescence²⁰ as well as the EPR results¹⁵ and extended X-ray absorption fine structure analysis¹² suggest that the role of Mn in its preferred lattice site is quite different from Cu and Ag as a dopant in the $\text{Li}_2\text{B}_4\text{O}_7$ lattice, and possibly reflects a multivalent Mn ion, as supported by the more recent structural studies.¹²

While it is very clear that conduction of the Li^+ ions occurs with great facility along the (001) direction,²⁻⁴ is there a similarly facile channel for Mn^{2+} and Mn^{3+} dopant in the $\text{Li}_2\text{B}_4\text{O}_7$ lattice?²¹

The $\text{Li}_2\text{B}_4\text{O}_7:\text{Mn}$ single crystals, with the natural isotope abundance (^6Li —7.4%, ^7Li —92.6%, ^{10}B —19%, ^{11}B —81%, and ^{55}Mn —100%), were grown from the melt by the Czochralski technique as described elsewhere.^{12,22-24} In the growth process of the $\text{Li}_2\text{B}_4\text{O}_7:\text{Mn}$ single crystals, we used

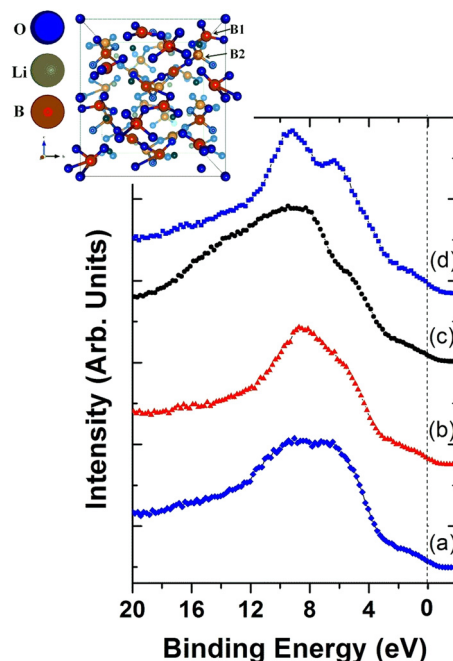


FIG. 1. The valence band photoemission spectra obtained for Mn doped $\text{Li}_2\text{B}_4\text{O}_7$ at a temperature of (a) 25°C , (b) 115°C , (c) 215°C , and (d) cooled back to 25°C . The photoelectrons were collected normal to the sample surface with an incident photon energy of 110eV . To correct for charging, the binding energies are relative to the valence band maximum.

MnO₂ added into the Li₂B₄O₇ melt at a 0.4% molar concentration, i.e., 4-valence manganese (Mn⁴⁺) was the initial starting point. The single crystal Li₂B₄O₇:Mn samples are nominally Li_{1.95}Mn_{0.05}B₄O₇, as determined by quantitative spectrographic analysis. The manganese appears to reduce to Mn²⁺, bivalent, in the Li₂B₄O₇:Mn lattice.

Angle-resolved photoemission spectra were obtained using plane polarized synchrotron light dispersed by a 3 m toroidal grating monochromator,^{25,26} at the Center for Advanced Microstructures and Devices (CAMD).²⁷ The measurements were made in an ultra-high vacuum (UHV) chamber employing a hemispherical electron analyzer with an angular acceptance of $\pm 1^\circ$, as described elsewhere.^{25,26} The combined resolution of the electron energy analyzer and monochromator is 150 meV for the photon energy of 110 eV. The photoemission experiments were undertaken with a light incidence angle of 45° with respect to the surface normal, unless stated otherwise. The photoelectrons were collected at emission angles as stated with respect to the surface normal throughout. The sample was sputtered using an Argon beam for 15 min at a voltage of 2.0 kV and annealed to remove surface contaminants prior to the measurements.

The spectra are aligned to the valence band maximum, and all binding energies reported here are relative to that valence band maximum. To determine the extent of charging, the valence band maximum has been referenced to the Fermi level established relative to a gold foil in contact with the sample. The measurements at elevated temperature of 350 °C were used as a reference, where little or no photovoltaic charging was observed in these or other samples.¹

Mn segregation is evident from the Mn 3p shallow core level in Figure 2. The photoemission spectra in the region of the Li 1s and Mn 3p obtained for Mn doped Li₂B₄O₇ show the presence of Mn at 25 °C and 115 °C, evident from the Mn 3p shallow core level, which appears here at a binding

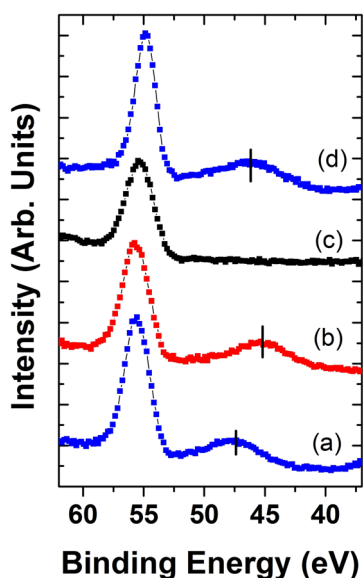


FIG. 2. The photoemission spectra in the region of the Li 1s and Mn 3p, obtained for Mn doped Li₂B₄O₇ obtained at a temperature of (a) 25 °C, (b) 115 °C, (c) 215 °C, and (d) cooled back to 25 °C. The photoelectrons were collected normal to the sample surface with an incident photon energy of 110 eV. To correct for charging, the binding energies are relative to the valence band maximum.

energy of 47.3 ± 0.2 eV with respect to the valence band maximum. The Mn 3p shallow core level photoemission feature disappears at 215 °C but reappears upon cooling the sample back to 25 °C. Local strain is certainly expected with Mn doping at both the boron and lithium sites,¹² and surface segregation would provide a mechanism for strain relief.²⁸ This strain relief would diminish significantly at temperatures above 400 K, due to lattice expansion.⁴

The valence band of the Li_{1.95}Mn_{0.05}B₄O₇(001), after correcting for charging, is seen to vary with temperature, as shown in Figure 1. Although Mn segregation to the surface is implicated, the spectral features of the valence band region are roughly 2 eV greater binding energies than the similar features observed for the manganites²⁹ and at least 1 eV greater than observed for MnO.³⁰ This greater binding energy is not easily attributed to a surface to bulk core level shift as the valence band features do appear at higher binding energies than observed for MnO films on Ag(100).³⁰ Likely, the valence band features are dominated at low temperatures by a surface Mn in a very high oxidation state, while at higher temperatures, the valence band spectrum is likely more representative of Li₂B₄O₇(001).

The assumption that the surface is dominated by manganese in a very high oxidation state is difficult to reconcile with the superficial assignment of the Mn 3p binding energy to 47.3 ± 0.3 eV, which is close to the expected value of 47.2 eV for metallic manganese. But the accuracy of the binding energies here are suspect because of the massive surface voltaic charging for Li_{1.95}Mn_{0.05}B₄O₇(001), larger than observed for other lithium tetraborate samples, as seen in Figure 3. Furthermore, the Mn 3p shallow core level binding energy shifts upon annealing. This change in the Mn core level binding energy with temperature could either be the

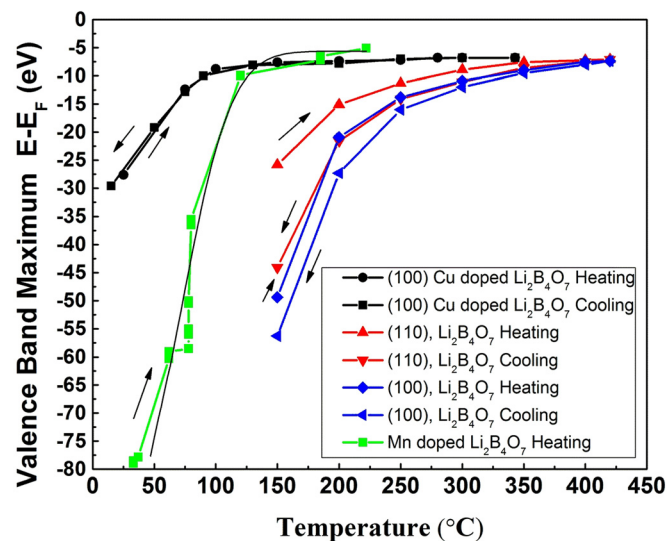


FIG. 3. The photovoltaic charging of Cu doped Li₂B₄O₇ (100) or Li_{1.998}Cu_{0.002}B₄O₇ (100) (black), Li₂B₄O₇ (110) (red), Li₂B₄O₇ (100) (blue), and Mn doped Li₂B₄O₇(001) or Li_{1.95}Mn_{0.05}B₄O₇ (001) (green) as measured from the position of the Fermi level, established using a gold foil, at temperatures in the region of 350 °C and above (to suppress surface and photovoltaic charging). Spectra were taken from a succession of temperatures using a photon energy of 56 eV, with electrons collected along the surface normal, except Mn doped Li₂B₄O₇ where a photon energy of 110 eV was employed. The Cu doped Li₂B₄O₇ surface charging data were adapted from Ref. 34, while the data for undoped Li₂B₄O₇ were adapted from Refs. 1 and 36.

result of manganese reduction, or an increase in screening in the photoemission final state as a result of increased coordination or better surface conductivity at higher temperatures. Several factors need to be considered, however. Here, the binding energies are with respect to the valence band maximum, not the Fermi level, because of the uncertainties in the assignments of the Fermi level in the presence of significant surface charging. This means that the binding energies are higher than are apparent. While the Li 1s core level binding energy (Figure 2) is close to the value of 55.7 eV reported for $\text{Li}_2\text{B}_4\text{O}_7$,³¹ values measured against an established Fermi level, at elevated temperatures where the surface charging is suppressed, are higher at 56.5 ± 0.4 eV,³² indicating that assigning the binding energies with respect to the Fermi level (adding roughly 3 eV to the binding energies reported here) means that a heavily oxidized Li and Mn surface species is now much more likely. An increase in Mn K edge absorption energy reported,¹² consistent with the 9.8 eV band gap of $\text{Li}_2\text{B}_4\text{O}_7$, is also indicative of an oxide and Mn within an oxygen coordination sphere, not a metallic Mn inclusion.

The driving force for segregation might not simply be strain relief along the $\text{Li}_2\text{B}_4\text{O}_7(001)$ direction. $\text{Li}_2\text{B}_4\text{O}_7(001)$ exhibits strong pyroelectric properties,³³ and both Li^+ and Mn^{2+} compensation of the pyroelectric surface charge is possible, but in fact Mn segregation occurs on both heating and cooling the crystal, and is rather present below 400 K. Thus, surface charge compensation cannot be the dominant mechanism driving surface segregation.

As seen in Figure 3, the surface photovoltaic charging is nearly completely suppressed by 120 °C. The decrease in surface photovoltaic charging saturates at a temperature far less than the 345 °C annealing temperature needed to suppress surface charging for the undoped lithium tetraborate.¹ The temperature required for complete suppression of surface photovoltaic charging remains at a somewhat more elevated temperature than the equivalently doped $\text{Li}_2\text{B}_4\text{O}_7:\text{Cu}$,³⁴ as illustrated in Figure 3. We need to bear in mind that for the Cu doped $\text{Li}_2\text{B}_4\text{O}_7$, the dopant atoms not only lead to Cu^+ ($3d^{10}$) and Cu^{2+} ($3d^9$) ions substituting for lithium but also Cu^+ ions at interstitial sites,³⁵ while Mn can adopt an extremely high oxidation state unlike copper and lithium. On the other hand, for $\text{Li}_2\text{B}_4\text{O}_7:\text{Mn}$, the Mn dopants tend to favor the boron substitutional sites,¹² thus, ion conduction by Mn may be suppressed in comparison to ion conduction by Cu. Yet conductivity along the polar tetragonal (001) c axis is much higher than along the orthogonal (100) direction,⁴⁻⁶ so a comparison of the surface charging for the two dopants is fraught with difficulty until studies over a range of doping and crystallographic orientations are obtained.

What is clear though is that Mn doping does enhance conductivity over the undoped samples, and this is consistent with facile diffusion of Mn along some channel to and from the surface with changing temperatures. In fact, these results are consistent in the discontinuity in dielectric function reported previously for $\text{Li}_2\text{B}_4\text{O}_7:\text{Mn}$,²¹ in the region of 500 K, at temperatures lower than the discontinuity observed for the undoped lithium tetraborate along the c-axis.⁴

Overall, the data indicate that Mn segregates to the surface of $\text{Li}_{1.95}\text{Mn}_{0.05}\text{B}_4\text{O}_7(001)$ at low temperatures (at or

below 115 °C, at least), and that the bulk solubility increases with increasing temperature. This leads to a strong diminution of Mn segregation at elevated temperatures, but Mn segregation is re-established upon quenching the sample temperature back to room temperature (Figure 2).

This work was supported by the Defense Threat Reduction Agency (Grant Nos. HDTRA1-07-1-0008 and BRBAA08-I-2-0128), the NSF through the “QSPINS” MRSEC (DMR-0820521) at UNL, and STCU Project 4947. The views expressed in this article are those of the authors and do not reflect the official policy or position of the Air Force, Department of Defense or the U.S. Government. The authors are grateful to Natalia Lozova and Jim Petrosky for their technical assistance and advice.

- ¹V. T. Adamiv, Ya. V. Burak, D. Wooten, J. McClory, J. Petrosky, I. Ketsman, J. Xiao, Ya. B. Losovyj, and P. A. Dowben, *Materials* **3**, 4550 (2010).
- ²I. M. Rizak, V. M. Rizak, N. D. Baisa, V. S. Bilanich, M. V. Boguslavskii, S. Yu. Stefanovich, and V. M. Golovei, *Crystallogr. Rep.* **48**, 676 (2003).
- ³M. M. Islam, T. Bredow, and P. Heitjans, *J. Phys.: Condens. Matter* **24**, 203201 (2012).
- ⁴A. Senyshyn, H. Boysen, R. Niewa, J. Banys, M. Kinka, Ya. Burak, V. Adamiv, F. Izumi, I. Chumak, and H. Fuess, *J. Phys. D: Appl. Phys.* **45**, 175305 (2012).
- ⁵A. E. Aliev, Ya. V. Burak, and I. T. Lyseiko, *Izv. Akad. Nauk SSSR Neorg. Mater.* **26**, 1991 (1990).
- ⁶Ya. V. Burak, I. T. Lyseiko, and I. V. Garapin, *Ukr. Fiz. Zh.* **34**, 226 (1989).
- ⁷J. Krogh-Moe, *Acta Crystallogr.* **15**, 190 (1962).
- ⁸J. Krogh-Moe, *Acta Crystallogr.* **B24**, 179 (1968).
- ⁹M. Natarajan, R. Faggiani, and I. O. Brown, *Cryst. Struct. Commun.* **8**, 367 (1979).
- ¹⁰S. V. Radaev, L. A. Muradyan, L. F. Malakhova, Ya. V. Burak, and V. I. Simonov, *Kristallografiya* **34**, 1400 (1989); *Sov. Phys. Crystallogr.* **34**, 842-849 (1989).
- ¹¹Ya. V. Burak, B. V. Padlyak, and V. M. Shevel, *Radiat. Eff. Defects Solids* **157**, 1101 (2002).
- ¹²T. D. Kelly, L. Kong, D. A. Buchanan, A. T. Brant, J. Petrosky, J. W. McClory, V. T. Adamiv, Ya. V. Burak, and P. Dowben, “EXAFS and EPR analysis of the local structure of Mn-doped $\text{Li}_2\text{B}_4\text{O}_7$,” *Phys. Status Solidi B* (in press).
- ¹³B. V. Padlyak, W. Wojtowicz, V. T. Adamiv, Ya. V. Burak, and I. M. Teslyuk, *Acta Phys. Pol. A* **117**, 122 (2010).
- ¹⁴B. V. Padlyak, A. Drzewiecki, and O. O. Smyrnov, *Cur. Top. Biophys.* **33**(Suppl. A), 171 (2010).
- ¹⁵D. Podgórska, S. M. Kaczmarek, W. Drozdowski, W. Wabia, M. Kwasny, S. Warchoł, and V. M. Rizak, *Mol. Phys. Rep.* **39**, 199 (2004).
- ¹⁶V. M. Holovey, V. I. Lyamayev, M. M. Birov, P. P. Puga, and A. M. Solomon, *Funct. Mater.* **12**, 318 (2005).
- ¹⁷V. M. Holovey, V. I. Sidev, V. I. Lyamayev, and M. M. Birov, *J. Phys. Chem. Solids* **68**, 1305 (2007).
- ¹⁸A. Klemen, V. M. Holovey, and M. Ignatovich, *Radiat. Meas.* **43**, 375 (2008).
- ¹⁹A. T. Brant, B. E. Kananan, M. K. Murari, J. W. McClory, J. C. Petrosky, V. T. Adamiv, Ya. V. Burak, P. A. Dowben, and L. E. Halliburton, *J. Appl. Phys.* **110**, 093719 (2011).
- ²⁰K. P. Popovych, P. P. Puga, V. T. Maslyuk, V. M. Kraslynyec, V. M. Holovey, and G. D. Puga, *Acta Phys. Pol. A* **117**, 174 (2010).
- ²¹N. D. Baisa, V. S. Bilanich, V. M. Holovey, I. M. Rizak, V. M. Rizak, and S. Yu. Stefanovich, *Fiz. Tverd. Tela. (Phys. Solid State)* **48**, 1757 (2006).
- ²²Ya. B. Burak, V. T. Adamiv, I. M. Teslyuk, and V. M. Shevel, *Radiat. Meas.* **38**, 681 (2004).
- ²³V. T. Adamiv, Ya. B. Burak, I. V. Kityk, J. Kasperczyk, R. Smok, and M. Czerwinski, *Opt. Mater.* **8**, 207 (1997).
- ²⁴Ya. V. Burak, Ya. O. Dovgyi, and I. V. Kityk, *Fiz. Tverd. Tela (Phys. Solid State)* **31**, 275 (1989).
- ²⁵Y. Losovyj, I. Ketsman, E. Morikawa, Z. Wang, J. Tang, and P. Dowben, *Nucl. Instrum. Methods Phys. Res. A* **582**, 264 (2007).

- ²⁶P. A. Dowben, D. LaGraffe, and M. Onellion, *J. Phys.: Condens. Matter.* **1**, 6571 (1989).
- ²⁷J. Hormes, J. D. Scott, and V. P. Suller, *Synchrotron Radiat. News* **19**, 27 (2006).
- ²⁸M. Nagel, I. Biswas, H. Peisert, and T. Chassé, *Surf. Sci.* **601**, 4484 (2007).
- ²⁹*Surface Segregation Phenomena*, edited by P. A. Dowben and A. Miller (CRC Press, Boca Raton, FL, 1990).
- ³⁰D. N. McIlroy, C. Waldfried, J. Zhang, J.-W. Choi, F. Foong, S.-H. Liou, and P. A. Dowben, *Phys. Rev. B* **54**, 17438 (1996).
- ³¹A. Yu. Kuznetsov, A. V. Krzhalov, I. N. Ogorodnikov, A. B. Sobolev, and L. I. Isaenko, *Phys. Solid State* **41**, 48 (1999).
- ³²D. Wooten, I. Ketsman, J. Xiao, Ya. B. Losovyj, J. Petrosky, J. McClory, Ya. V. Burak, V. T. Adamiv, and P. A. Dowben, *Physica B* **405**, 461 (2010).
- ³³A. S. Bhalla, L. E. Cross, and R. W. Whatmore, *Jpn. J. Appl. Phys.*, **24**(Suppl. 24-2), 727 (1985). Available at <http://jjap.jsap.jp/link?JJAPS/24S2/727/>.
- ³⁴J. Xiao, N. Lozova, Ya. B. Losovyj, D. Wooten, I. Ketsman, M. W. Swinney, J. Petrosky, J. McClory, Ya. V. Burak, V. T. Adamiv, A. T. Brant, and P. A. Dowben, *Appl. Surf. Sci.* **257**, 3399 (2011).
- ³⁵A. T. Brant, D. A. Buchanan, J. W. McClory, P. A. Dowben, V. T. Adamiv, Ya. V. Burak, and L. E. Halliburton, "The origin of thermoluminescence in Cu-doped lithium tetraborate ($\text{Li}_2\text{B}_4\text{O}_7$) crystals," *J. Lumin.* **139**, 125 (2013).
- ³⁶D. Wooten, I. Ketsman, Jie Xiao, Ya. B. Losovyj, J. Petrosky, J. McClory, Ya. V. Burak, V. T. Adamiv, and P. A. Dowben, in *Nuclear Radiation Detection Materials*, edited by D. L. Perry, A. Burger, L. Franks, K. Yasuda, and M. Fiederle (Mater. Res. Soc. Symp. Proc., 2009), Vol. 1164, Paper No. L04-04.